Sādhanā (2018) 43:74
https://doi.org/10.1007/s12046-018-0831-0

Modelling and analysis of South Indian temple structures under earthquake loading

JETSON A RONALD[1], ARUN MENON[2,*], ANUMOLU MEHER PRASAD[2], DEVDAS MENON[2] and GUIDO MAGENES[3]

[1] Aon Benfield, Bangalore, India
[2] Department of Civil Engineering, Indian Institute of Technology Madras, Chennai 600 036, India
[3] Department of Civil Engineering and Architecture, University of Pavia, Via A. Ferrata 1, 27100 Pavia, PV, Italy
e-mail: ajetsonronald@yahoo.co.in; arunmenon@iitm.ac.in; prasadam@iitm.ac.in; dmenon@iitm.ac.in; guido.magenes@unipv.it

MS received 5 June 2017; revised 20 November 2017; accepted 4 January 2018; published online 11 May 2018

Abstract. The *gopuram* (multi-tiered entrance gateway) and the *mandapam* (pillared multi-purpose hall) are two representative structural forms of South Indian temples. Modelling and seismic analysis of a typical 9-tier *gopuram* and, 4- and 16-pillared *mandapam* of the 16th century AD Ekambareswar Temple in Kancheepuram, South India, are discussed. The seismic input is based on a probabilistic seismic hazard analysis of the archaeological site. Two modelling strategies, namely lumped plasticity and distributed plasticity modelling, and three analysis approaches, namely linear dynamic, non-linear, static and dynamic analyses were adopted for the seismic assessment of the *gopuram*. Unlike slender masonry towers, the vulnerable part of the *gopuram* could be at the upper levels, which is attributable to higher mode effects, and reduction in cross section and axial stresses. Finite element and limit analysis approaches were adopted for the assessment of the *mandapam*. Potential collapse mechanisms were identified, and the governing collapse of lateral load, calculated based on limit theory, was compared with the seismic demand as a safety check. Simple relations, as a means of rapid preliminary seismic assessment, are proposed for the *mandapam*.

Keywords. Dravidian temple structures; *gopuram*; *mandapam*; seismic vulnerability assessment.

1. Introduction

1.1 *The Dravidian style of temple architecture*

The configuration of the Hindu temple can be traced to the early Buddhist rock-cut sacred spots (*chaitya*) and monasteries (*vihara*), seen in Ajanta (2nd c. BC) for instance, while the earliest structural temples can be traced to the Gupta (e.g., Vishnu temple in stone, Deogarh, 500 AD; brick temple, Bhitargaon, 550 AD) and the Chalukya period from the 6th c. AD (e.g., Lad Khan and Durga temples, Aihole). Aihole in South India along with Pattadakal is considered as the experimental ground for the temple structure, where the transition from the northern *Nagara* style (identified by the *shikara*, the tower-like structure crowning the *garba griha*, the sanctum sanctorum) to the southern Dravidian style (identified by the *vimana*, stepped pyramidal structure ending in a dome over the *garbagriha*), in turn called the Vesara style, can be observed. The Dravidian style later evolved in South India under the Pallava, Chola, Pandya, Vijayanagara and Nayak dynasties until 18th c. AD. In its final form, every tier of the *vimana* is defined by horizontal mouldings, a derivative of the overhangs of thatch roof over bamboo huts. Described as the Dharmaraja vimana, which evolved during the Pallava rule (circa 7th c. AD), this was clearly based on the form of a Buddhist vihara. The Pallava shore temples of Mamallapuram, the Kailashnath (7th-8th c. AD) and Vaikunta Perumal Temples in Kancheepuram (720 AD), the Virupaksha Temple in Pattadakal (740 AD) of the Chalukyas and the Chola Brihadeswara Temples at Thanjavur and Gangaikondacholapuram (11th c. AD) are few examples.

1.2 *Description of the gopuram*

The multi-tiered archetypal entrance gateway in the Dravidian temple, the *gopuram*, was a feature introduced by the Pandyas in 14th c. AD in order to confer architectural status to structurally insignificant ancient shrines. A *gopuram*, typically rectangular in plan, rises as a truncated pyramid, which is crowned by a structure resembling the Buddhist

*For correspondence

chaitya with finials over its ridge. Structures such as the *gopuram* of the Meenakshi Temple in Madurai (1600 AD), Ranganathaswamy Temple in Srirangam (17^{th} c. AD) and Ekambareswar Temple in Kancheepuram, built by Vijayanagara rulers in 16^{th} c. AD, are ubiquitous and representatives of the highly evolved Dravidian temple architecture. Among the several *gopuram* in a temple, the tallest is referred to as *Rajagopuram* (“raja” meaning king). The structure serves as a landmark as it can be sighted from great distances. The principal function of the gopuram is to serve as a prominent entrance gateways to the premises, typically in the four cardinal directions. It is essentially a masonry tower, composed of an odd number of stories with a structural configuration similar to a bell tower or a minaret. Their structural responses are comparable. Several researchers have investigated the response of such towers to seismic loads [1–7].

A representative 9-tier *gopuram* (see figure 1a) was chosen from Ekambareswar temple in Kancheepuram, built by Krishnadevaraya (16^{th} c. AD). The temple is one of the most ancient shrines dedicated to Shiva, and has apparently been in existence even prior to 7th c. AD. Pillars with inscriptions of Mahendravarman I, the Pallava king, who ruled from 610-630 A.D., were discovered in here [8]. Several additions were carried out by Pallava, Chola and Vijayanagara dynasties to the ancient shrine over the centuries.

The *gopuram* is rectangular in plan (see figure 2) with base dimensions of 25 m by 18 m and floor area reducing with height. Internal staircases are present. The *gopuram* rises to a height of 48.4 m. The foundation is not more than 3 m deep, and consists primarily of random rubble masonry. The ground storey walls are of multi-leaf stone masonry construction, with dressed granite blocks and an inner core of rubble masonry. The remaining stories are made up of burnt clay brick masonry. The floor slabs are of the Madras terrace system, with closely spaced wooden rafters spanning the walls, supporting bricks arranged diagonally in a brick-on-edge style, topped with brick bats and lime mortar, a system that a flexible diaphragm under lateral loading. The exterior of the *gopuram* is decorated with sculptures in reinforced mortar derived from Hindu mythology.

1.3 *Description of the mandapam*

The *mandapam* or a multi-purpose pillared hall is a common archetypal feature of the Dravidian temples. The *mandapam* originated as an antechamber to the *garbagriha* in the spatial hierarchy in a temple. It was in Virupaksha Temple at Pattadakal, built by Chalukyas, that the metamorphosis of the *mandapam* as a more convincing spatial linkup between various hierarchical spaces of a Hindu temple was observed [9]. Later, it evolved as a multipurpose architectural composition with a myriad of intricately carved columns (e.g., thousand-pillared hall, Meenakshi Temple in Madurai).

The *mandapam* in its simplest form is either a free-standing entity within a temple complex or attached to the principal structure. The structure is constituted by the rudimentary post and lintel members. Important temples usually have a number of *mandapams*, each intended for a different function, such as conduct of rituals, performing arts, resting spot for devotees, etc. The structural members are the pillars (made up of a pedestal, monolithic shaft and capital), the corbels and the beams. These members in stone

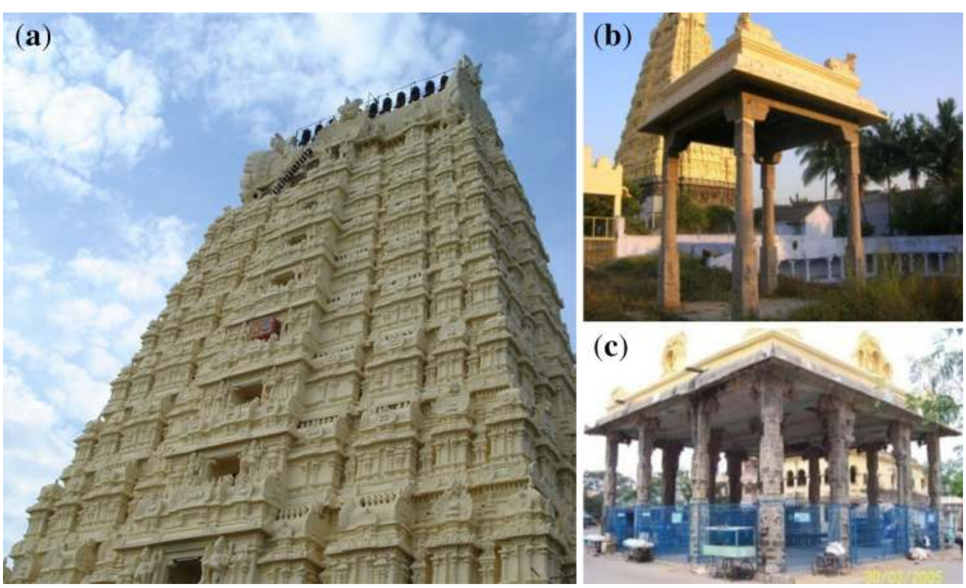

Figure 1. (**a**) 9-tiered *gopuram*, (**b**) 4-pillared *mandapam* and (**c**) 16-pillared *mandapam* of Ekambareswar Temple in Kancheepuram, 16^{th} c. A.D.

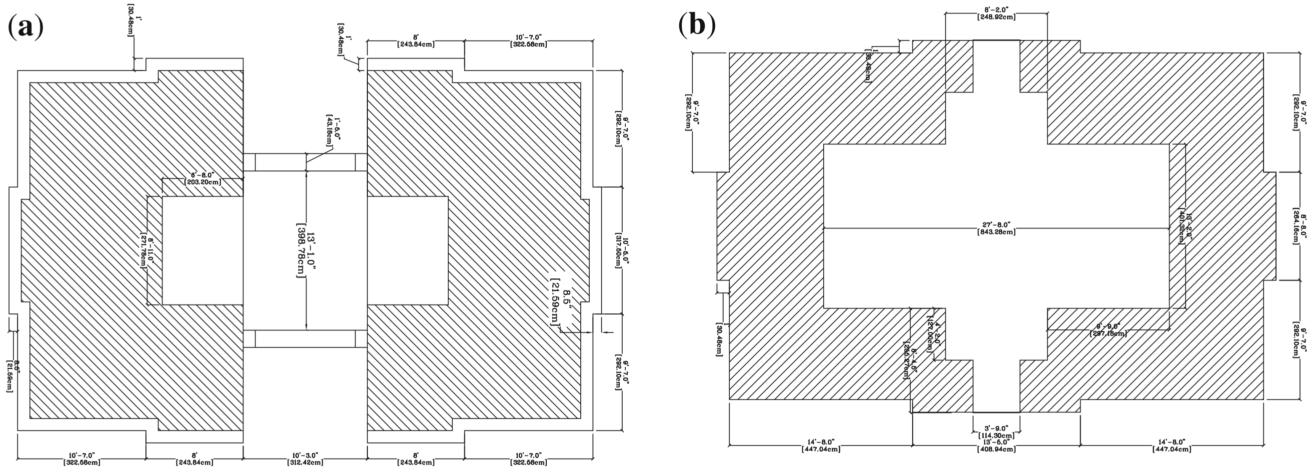

Figure 2. Typical configuration of a *gopuram* in plan: (**a**) ground storey, (**b**) upper stories.

may be connected to each other through a tenon-mortise joint, with or without lime mortar at the interface. In South Indian architecture, the stone members merely rest against each other with no interlocking mechanism. Wide cornices and sunshades resting on the beams are seen in some *mandapams*, which are held in place, by the weight of overlying merlons or parapets. Typical pillar spacing varies from 2 m to 3 m. The roof of the *mandapam* is made up of stone slabs spanning between beams, packed with lime mortar.

Four typical *mandapams* at Ekambareswar temple were considered for the study. These consist of 16-pillared and 4-pillared structures, each 3 m and 7 m in height. A 3 m high 4-pillared *mandapam* and a 7 m high 16-pillared *mandapam* are shown in figure 1(b)_(c).

1.4 *Seismic vulnerability of historical structures*

Inadequacies in historical masonry buildings in active seismic regions in India were noticed in the Bhuj earthquake in 2001 [10]. Although seismic hazard of South India is lower than the north, the heritage value of these structures demands detailed assessment to identify highly vulnerable heritage stock and to develop risk mitigation strategies.

Common problems in masonry towers (e.g., *gopurams*) under seismic loading emerge from material characteristics, slenderness effect, lack of redundancy and the construction typology. These structures, which are often slender and tall, being flexible, could attract lower seismic forces. But their increased height increases the lever arm for overturning moment due to lateral forces and hence, the slenderness effect could have adverse consequences. Inclination of ancient towers, primarily due to differential soil settlement, is common. Hence, the resulting secondary stress could be large [2]. Multi-leaf construction is a common typology, often resorted to so as to increase wall thickness and counter gravity loads. With homogenous infill and adequate interconnections between veneers, such a system could be stable under static loads, but not necessarily under dynamic loads. Increased thickness implies higher mass, not higher resistance. Disintegration of the infill masonry and deterioration of the interconnection between veneers are very common in ancient masonry walls leading to increased vulnerability under lateral loads.

In *mandapams*, the lime mortar that provides an interface between pillars, corbels and beams offer no resistance to tension. Hence, during ground motion they are expected to behave like dry masonry structures. *Mandapams* are comparable to the Roman classical single drum columns with architraves (e.g., Parthenon Pronaos, Greece). The slenderness effect of the monolithic pillar makes the structural behaviour of the *mandapam* considerably different from that of classical multi-drum Greek temple structures. Studies on the porch of Parthenon [11, 13] reveal that seismic response of such structures is sensitive to the structural configuration, as well as ground motion parameters, with their dynamic behaviour being highly non-linear. Collapse of these structures is mainly due to instability rather than exceedance of material strength [11, 12, 14]. Hence, assessment methods that give due importance to the geometry are required.

2. Methodology adopted

The structural system of the *gopuram* was reconstructed based on inputs from temple architects, and details were verified with in-situ inspections. The seismic input at the archaeological site was defined through a parallel study. Probabilistic Seismic Hazard Assessment (PSHA) and stochastic site response analysis based on in-situ and laboratory, geophysical and geotechnical experiments to characterize the sub-soil were carried out to define the seismic input in terms of acceleration spectra and suites of acceleration records to perform time-history analysis. A 3D finite element (FE) model of the *gopuram* was developed for gravity and response spectrum analyses, while non-linear analyses, both static and dynamic, were performed using a lumped mass model, with distributed plasticity. The seismic vulnerability of *mandapams* was studied by two approaches: linear FE approach and a simplified non-linear approach based on limit analysis.

Ambient vibration tests were executed to identify the fundamental frequency of the *mandapams*, and subsequently, the findings were used to calibrate FE models. However, during the simulation very high frequency values were obtained for the models with elastic modulus (E) estimated from experimental tests on material samples. Subsequently, the E value was reduced to around $1/10^{th}$ its original, in order to match ambient vibration test results, suggesting FE continuum modelling for dry masonry is not appropriate. Researchers have come to similar conclusions on FE modelling of dry masonry towers in Bayon temple, Cambodia [15].

Several challenges are encountered in structural assessment of historical buildings due to: (1) lack of material characterization and peculiarities of the materials used, (2) poor understanding of ancient construction practices, especially sequence of construction, (3) existing damages and difficulty in diagnosing these, and (4) lack of code provisions for structural assessment. Often these setbacks render sophisticated analysis less reliable. Simplified analysis is generally adopted as an alternative, or prior to rigorous analysis for recurrent structures mainly to identify the most vulnerable configurations and to prioritize retrofitting schemes [16]. Such approaches are effective for symmetrical structures with simple configurations. A similar approach has been adopted here. The structures selected for the present study are representative samples of recurrent forms in South Indian temples. A simplified procedure based on limit analysis has been proposed, which gives factor of safety as a function of the peak ground acceleration (PGA).

3. Definition of the seismic input at Kancheepuram

3.1 *PSHA of the archaeological site*

Indian seismicity is characterized by a relatively high frequency of large earthquakes and a relatively low frequency of moderate ones. The zoning map of India divides the country into four seismic zones, namely zone II (MSK intensity VI), III (MSK VII), IV (MSK VIII) and V (MSK IX or more). The assigned effective PGA corresponding to the Maximum Considered Earthquake (MCE) are 0.36 g (zone V), 0.24 g (IV), 0.16 g (III) and 0.10 g (II) [17]. Since the occurrence of recent moderate earthquakes in Peninsular India, such as the M_w 6.4 Latur earthquake (1993) and the M_w 5.5 Pondicherry earthquake (2001), Peninsular India has been considered to be moderately active. PSHA at the archaeological site in Kancheepuram was performed using an earthquake catalogue for the region from 1507-2007 AD. More information on the hazard analysis can be obtained from [18] and [19].

PGA for different return periods are tabulated (table 1) and the uniform hazard acceleration spectra are shown in figure 3 (a)–(b). From deaggregation analysis of PSHA results, the controlling earthquake at Kancheepuram, for the PGA with 475-year return period is an event of magnitude M_w 4.0-5.2 and hypocentral distance 17-31 km. Suites of seven natural acceleration records on rock sites from worldwide strong motion databases were identified by imposing spectrum-compatibility criterion between the mean spectrum of the selected records and the uniform hazard spectrum from the PSHA study [20, 21] stipulates at least seven records for average response quantities from non-linear time-history analyses. Scaling factors used to match the PGA (e.g., for the 2475-year return period) vary between 0.45 and 2.8 (refer table 2). The records selected for the 2475-year return period event are shown in figure 4.

3.2 *Experimental investigations*

Sub-soil characterization at the site was carried out using invasive (standard SPT) and non-invasive geophysical procedures (MASW technique). The most important dynamic parameter, which affects the damage levels in the structure i.e., the fundamental frequency of the site, was estimated experimentally (see table 3). Dynamic impedances that characterize the soil have been computed for soil-structure interaction (SSI) analysis, considered in the assessment of the *gopuram*. Dynamic spring (stiffness) constants and dashpot (damping) constants have been calculated based on the geometry of the foundation as well as

Table 1. Peak ground accelerations from PSHA compared to IS code [17, 19].

Probability of exceedance	Return period (Years)	PSHA		IS – 1893-1 (2002)	
		PHA* (g)	PVA* (g)	PHA (g)	PVA (g)
2% in 50 years	2475	0.141	0.067	0.16	0.11
5% in 50 years	975	0.105	0.049	-	-
10% in 50 years	475	0.080	0.037	0.08	0.05
40% in 50 years	95	0.041	0.021	-	-

* PHA – peak horizontal ground acceleration; PVA – peak vertical ground acceleration

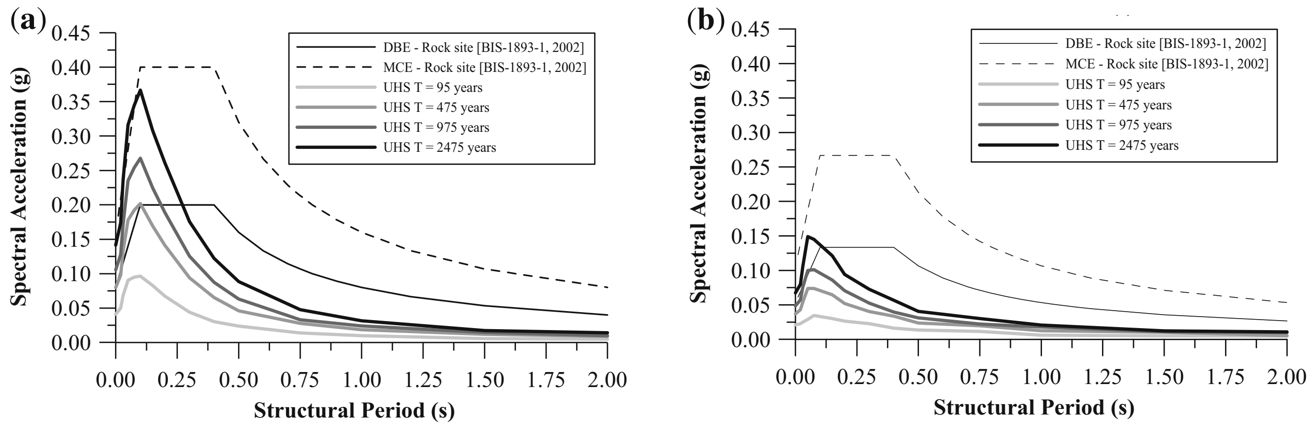

Figure 3. Uniform hazard spectra compared to the elastic response spectra from [17] for (**a**) horizontal ground motion; (**b**) vertical ground motion [19].

mechanical properties of the subsoil, as reported in table 4, using the dynamic impedance model [22].

4. Analysis of the *gopuram*

4.1 *Material model*

A limited number of tests were carried out for estimating the mechanical properties of the construction materials of the *gopuram*. These tests were conducted on samples procured from the distressed portions of similar structures in the temple. Dynamic identification with ambient vibration is not appropriate for large structures, such as the *gopuram*, due to high background noise. Recourse to forced dynamic tests with harmonic vibration is required, considering the size and complexity of the structure, which could not be executed in the current study. Since the objective of the study was to understand the global behaviour of the structure, the macro-modelling approach was adopted. Homogenization of masonry was carried out on the lines of available models in the literature [23–26]. However, none of these are specific to historical masonry, but focus on typical masonry constructions in India. Based on the limited mechanical tests performed on material samples, elastic properties of brick and stone masonry were conservatively assumed (refer table 5). The tensile strength of the masonry was ignored due to ageing effects and deterioration. The material model used in the study was proposed by [27] and [28] for masonry towers, which is based on the premise that compression failure mode is not purely brittle. As seen in figure 5, the model is capable of capturing both negative and degrading stiffness. Degradation depends on the maximum plastic strain occurring during the loading history. Local collapse for a single fibre is defined when a certain value of maximum strain in compression is reached, after which the fibre cannot contribute anymore to the sectional resistance.

4.2 *Structural modelling*

4.2a *3D Finite Element Model*: Gravity load analysis and response spectrum analyses were carried out using 3D FE model. Only members meant to carry loads were modelled. The floor diaphragms are very flexible and poorly connected to the walls, hence not modelled. Openings in the walls were modelled. The foundation was modelled using the dynamic spring and damping constants to account for SSI. FE modelling was carried out on an ABAQUS 6.6.4 platform. C3D10, a 3D tetrahedron continuum element with 10 nodes and quadratic displacement behaviour was used in the model. Each node has three degrees of freedom in the nodal x, y and z directions. The tetrahedron element was preferred because of the irregular geometry of the structure.

4.2b *Lumped mass model*: 3D models become difficult to deal with when the type of analysis to be performed is iterative or when a large number of analyses have to be carried out. A lumped mass or "stick" model is effective for symmetric structures and is used as an alternative to 3D FE models. 3D beam-column elements capable of accounting for geometric and material non-linearity were used. A limitation of this element is that shear deformations are ignored. However, shear response may be not a dominating mechanism in these tall slender structures. The mass of the structure is represented by single-node lumped mass elements, characterised by three translational and three rotational inertia values. Non-linear analysis was performed with this model.

4.2c *Modelling inelasticity*: Two approaches are commonly used to study the inelastic behaviour of structures viz. concentrated plasticity and distributed plasticity approaches. The former works well for capacity designed structure, or for structures where locations of inelastic regions are known *apriori*. Such a choice is impractical in historical masonry structures. The latter overcomes this difficulty, but they could be computationally demanding. In the present

Table 2. Seismological characteristics of the suite of natural accelerograms.

#	Record ID	Earthquake	M_w^4	Epicentral distance (km)	Depth (km)	Fault type	Station[1]	Unscaled PGA (m/s^2)	Unscaled PGV (cm/s)	PGA Scaling factor[3]
1.	000284X[2]	El Asnam, Algeria, 1980	4.75	24	3	Thrust	Beni-Rashid, Algeria	0.481	1.871	2.84
	-							-	-	-
	000284Z							0.131	1.807	5.01
2.	000854X	Umbria-Marche, Italy, 1998	5.10	21	6	Unknown	Gubbio-Piana, Italy	0.529	3.113	2.80
	000854Y[2]							0.494	3.636	2.80
	000854Z							0.253	1.436	2.60
3.	000857X[2]	Umbria-Marche, Italy, 1998	4.90	10	10	Unknown	Nocera Umbra, Italy	1.710	3.578	0.81
	000857Y							1.424	3.595	0.81
	000857Y							0.635	1.196	1.03
4.	000852X	Umbria-Marche, Italy, 1998	5.10	11	6	Unknown	Nocera Umbra, Italy	3.907	9.964	0.45
	000852Y[2]							2.771	8.890	0.45
	000852Z							1.250	2.618	0.89
5.	000853X[2]	Umbria-Marche, Italy, 1998	4.90	11	10	Unknown	Nocera Umbra-Biscontini, Italy	0.959	1.444	0.65
	000853Y							2.109	6.363	0.65
	000853Z							0.481	1.164	1.37
6.	000457X[2]	Spitak, Armenia, 1988	4.74	10	5	Unknown	Toros, Armenia	1.702	3.837	0.82
	000457Y							1.047	2.583	0.82
	000457Z							0.553	0.870	1.19
7.	0098X[2]	Hollister-03, California, 1974	5.14	11.08	6.1	Strike-slip	CDMG 47379, Gilroy array #1, CA	1.149	3.150	1.34
	0098Y							1.299	-	1.34
	-							-	-	-

NOTE:

1. All records pertain to stations situated on rock sites and in the free-field.

2. Horizontal acceleration record selected by imposing spectrum-compatibility criterion with 475-year return period UHS from the PSHA. The horizontal PGA scaling factor pertains to these records.

3. The orthogonal horizontal component is scaled to the same scaling factor as in 2, while the vertical component is scaled to the vertical PGA from the PSHA (0.657 m/s^2).

4. Calculated from other magnitude measures.

5. Records 1-6 are from the ESMD (http://www.isesd.cv.ic.ac.uk/ESD/frameset.htm) and record 7 is from the PEER NGA (http://peer.berkeley.edu/nga/). Records 2-6 pertain to aftershocks.

study, a distributed plasticity approach has been adopted, as the structure is simple with few elements. Fibre element modelling, which does not require explicit definition of a moment-rotation relationship, has been used. Only the sectional geometry and the material constitutive law require to be assigned.

4.2d *Modelling damping*: Defining reliable damping parameters are paramount in non-linear analysis. Damping due to the inelastic material behaviour is automatically taken care of by the material model but for the other sources of damping, generally a viscous damping approach is followed. The Rayleigh damping approach was adopted here. The damping ratio was considered to be 2%-3% for the period range of 0.3-1.0 s, which was determined from modal analysis. In the selected range of periods, the cumulative modal mass contribution is more than 90%. The damping ratio was selected from the literature on similar structures [29, 30]. The stiffness considered was a tangent stiffness, which updates itself at every time step.

4.3 *Elastic analysis*

4.3a *Modal analysis*: Modal analysis was performed in order to identify the dynamic characteristics of the structure. The frequencies, modes of vibration, modal mass and their cumulative ratio are listed in table 6, and mode shapes are shown in figure 6. The fundamental mode is associated with bending in the principal directions. First two mode frequencies are close though the structure is rectangular in plan (1.3 Hz, 1.6 Hz). Large openings along the wall reduce the stiffness in the longer direction. Modal analysis confirms the importance of higher modes, because the masses associated with fundamental modes are only around 60-70%. The natural period falls in the descending branch of the response spectrum, a feature inherent to tall masonry towers.

The dynamic properties of the *gopuram* are comparable with other ancient masonry towers, e.g., natural frequencies of Qutb minar [30], Minaret of Jam, Afghanistan [31] and a multi-tiered Nepalese temple [29] are 0.80 Hz, 0.94 Hz and 1.68 Hz, respectively.

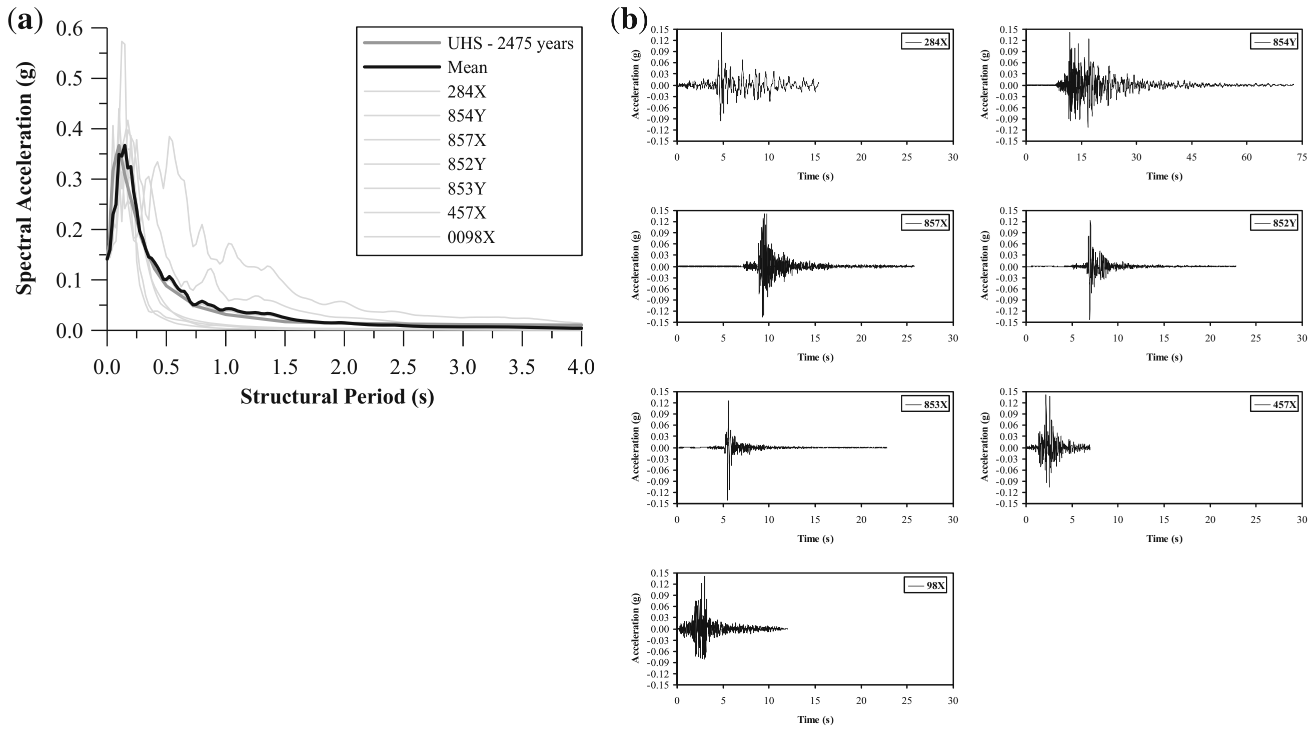

Figure 4. (**a**) Probabilistic UHS for 2475-year return period, individual spectra of 7 spectrum-compatible natural records (on rock) and their mean response spectrum; (**b**) Time-histories of 7 selected records.

Table 3. Site characteristics from experimental investigations.

Investigation method	Shear wave velocity (m/s)	Frequency of site (Hz)
Bore hole test	379	3.79
MASW	348	3.48

Table 4. Dynamic impedances for soil-structure interaction.

Degree of freedom	Stiffness Coefficient (kN/m)	Damping Coefficient (kNs/m)
Z	1.27.E+07	7.80.E+05
Y	1.03.E+07	4.71.E+05
X	9.97.E+06	4.45.E+05
θX	3.83.E+09	8.82.E+07
θY	8.39.E+09	1.94.E+08
θZ	1.69.E+09	3.99.E+07

Table 5. Dynamic impedances for soil-structure interaction.

Investigation method	Compressive strength (MPa)	Modulus of elasticity (MPa)	Poisson's ratio
Brick masonry (*gopuram*)	2.5	2000	0.10
Stone masonry (*gopuram*)	5.0	4000	0.10
Stone (mandapam)	50.0	7000	0.10

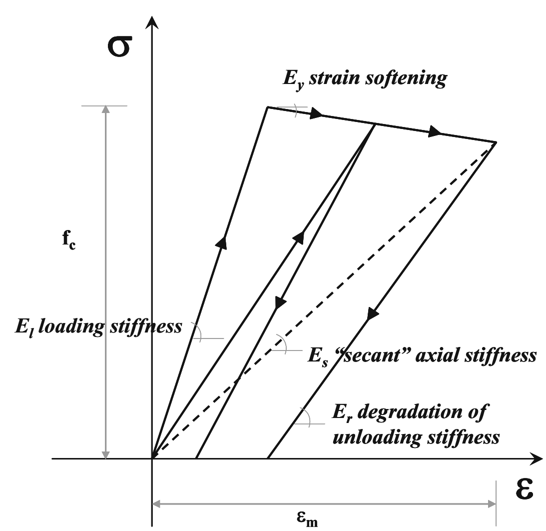

Figure 5. Stress-strain relation for axial material response of historical masonry used in fibre modelling with tensile strength neglected (after [28]).

4.3b *Response spectrum analysis*: The *gopuram* was analysed using the site-specific uniform hazard spectra. In the current research, the structure is analysed to ground motion with a 40% probability of exceedance in 50 years or a 95-year return period (frequent event), a 10% probability of exceedance in 50 years or a 475-year return period (rare event), as well as, ground motion with a 2% probability of

Table 6. Dynamic properties of the *gopuram* from 3D FE model.

			Effective modal mass			Cumulative modal mass		
Mode	Frequency (Hz)	Mode of vibration	Ux	Uy	Uz	Ux	Uy	Uz
1	1.30	B - XX	0.64	0.00	0.00	0.64	0.00	0.00
2	1.60	B - YY	0.00	0.57	0.00	0.64	0.57	0.00
3	3.40	Torsional	0.00	0.00	0.00	0.64	0.57	0.00
4	3.50	Vertical	0.00	0.00	0.98	0.64	0.57	0.98
5	3.80	B - XX	0.28	0.00	0.00	0.92	0.57	0.98
6	4.10	B - YY	0.00	0.33	0.00	0.92	0.90	0.98

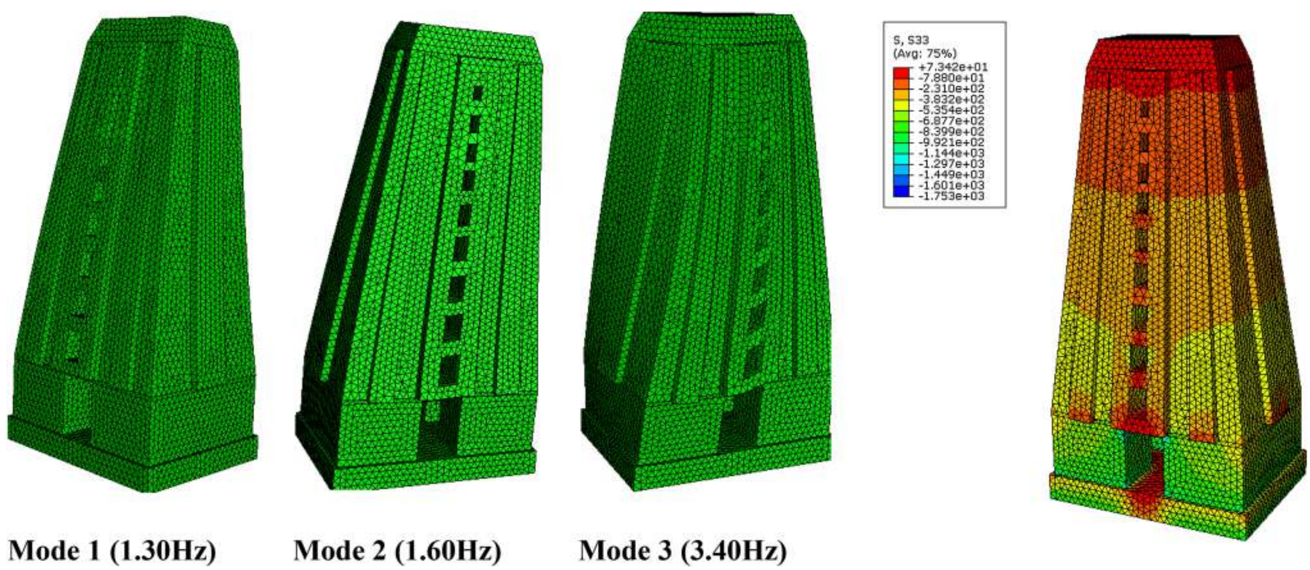

Figure 6. Mode shapes and stress contours from gravity load analysis from 3D FE model of the 9-tiered *gopuram*.

exceedance in 50 years or a 2475-year return period (very rare event). The resulting stress distribution was calculated by superimposing the stress resulting from gravity load with that from the response spectrum analyses (see figure 7).

Masonry structures are typically meant to resist compressive forces, and tensile forces are to be avoided as far as possible. The code of practice for structural use of unreinforced masonry [32], allows only 0.1 MPa of tensile stress. Under service loading, development of any amount of tensile stress is a matter of concern. The structure develops significant tensile stress ($\approx$ 0.1 MPa) for higher return periods, but almost no tensile stress for the Design Basis Earthquake (DBE). Maximum tensile stress is noticed at higher levels (near 7th floor), and not at the base. This is attributable to a significant reduction of cross section with height with a correlated reduction of the beneficial axial compression, and also to higher mode contributions. Maximum compressive stress is within the section capacity for MCE too. The stress resultants are shown in figure 8.

4.4 *Non-linear analysis*

That non-linear dynamic analysis, commonly referred to as non-linear time history analysis (NTHA) is the most accurate method for studying seismic response of structures, is indisputable. However, the approach requires reliable seismic input and is computationally demanding. Therefore, it is not always the first choice and generally adopted to validate the results of the other non-linear approaches. An alternative approach is non-linear static (pushover) analysis. In the present study, pushover analysis was carried out so as to complement NTHA and also to verify its applicability to masonry towers. The non-linear analyses were performed using SeismoStruct v.4.0.9 [33], which adopts fibre element modelling with a stiffness-based formulation. The sectional stress-strain state of beam-column elements is obtained through the integration of the non-linear uniaxial material response of the individual fibres into which the section is subdivided, fully accounting for the spread of inelasticity along the member length and across the section depth. The member is also capable of

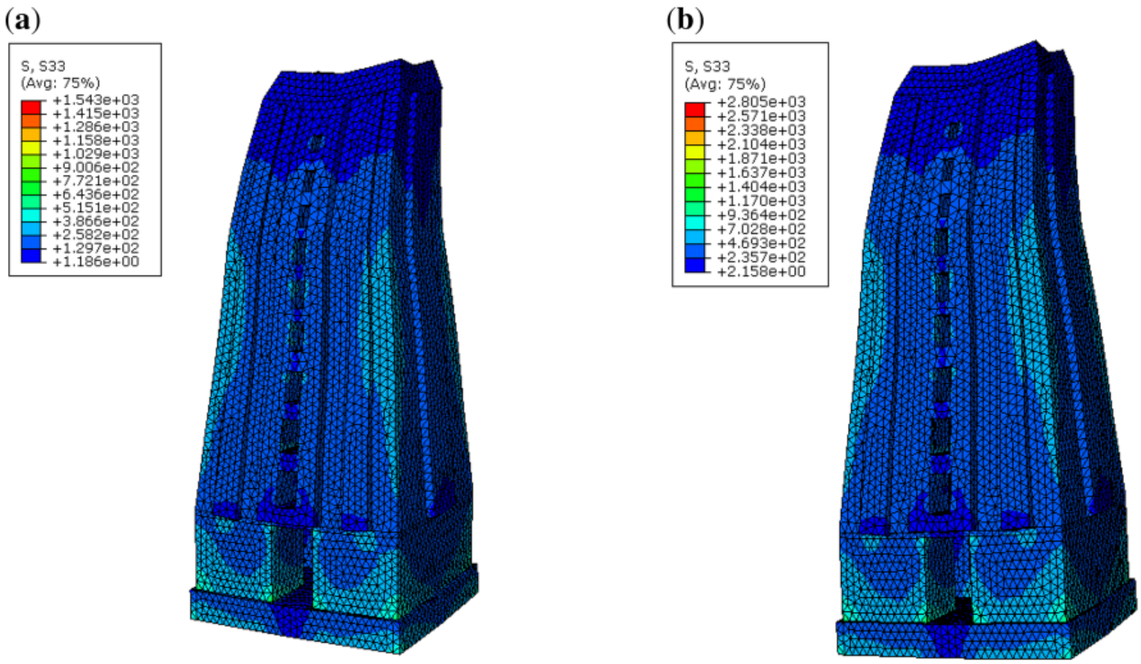

Figure 7. Stress contours for multi-modal response spectrum analysis from linear elastic 3D FE model (**a**) 475-year return period spectrum; (**b**) 2475-year return period spectrum (units KPa).

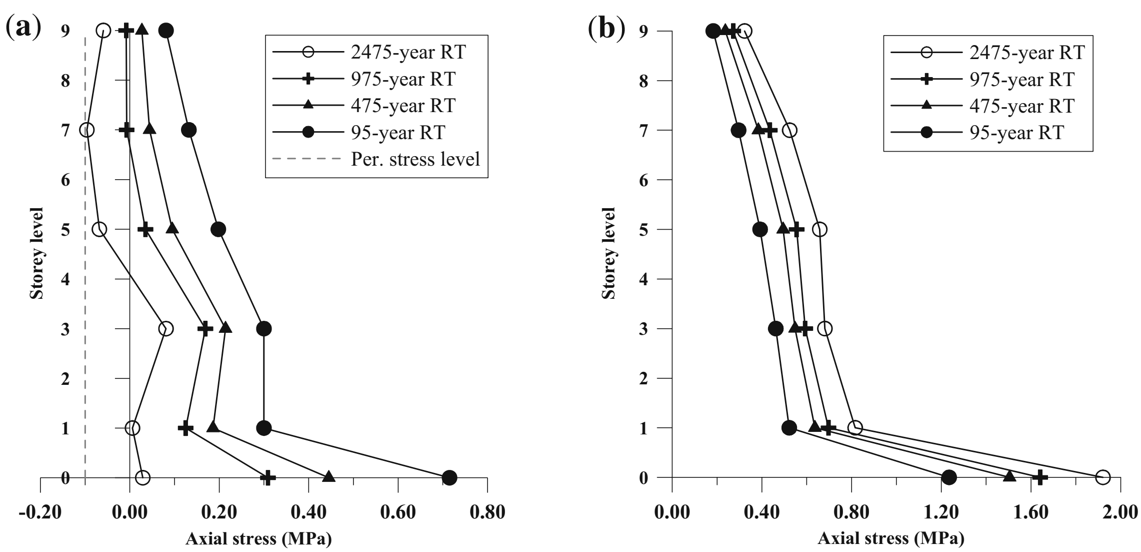

Figure 8. Stress resultant: (**a**) minimum stress; (**b**) maximum stress (stresses from gravity load analysis combined with response spectrum analysis (compressive stress: +ve).

accounting for local geometric non-linearity (beam-column effects).

4.4a *Non-linear static analysis*: Higher mode contribution is evident from modal and response spectrum analysis, a trend observed in other studies too [1, 2, 29, 30]. Since conventional pushover analysis is incapable of accounting for higher mode effects, the modal pushover analysis (MPA) [34] was adopted. MPA explicitly accounts for higher mode contributions, and this method is conceptually simple and computationally attractive. The load vector was assigned according to the shapes of the first three modes of vibration (see figure 9a) and the pushover curve was obtained for each distribution (see figure 9b). The lumped mass model was used to perform the pushover analyses.

The capacity curve thus obtained corresponds to the MDOF system, which is subsequently transformed to that of an equivalent SDOF system using standard procedures. The capacity spectrum method [35] was used to estimate

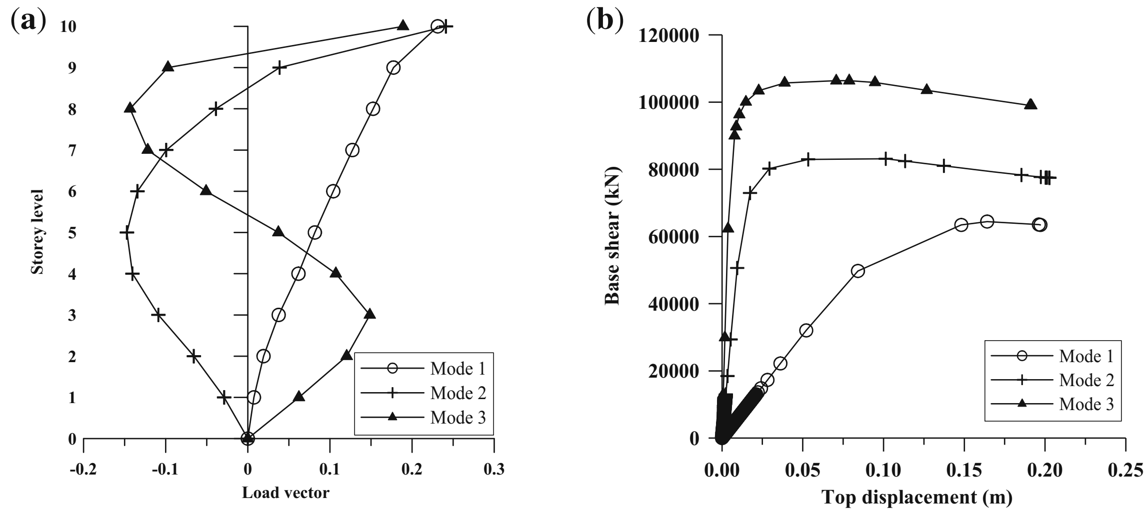

Figure 9. (**a**) Loading profiles for the three modes adopted for the MPA procedure; (**b**) individual pushover curves obtained for the three modes.

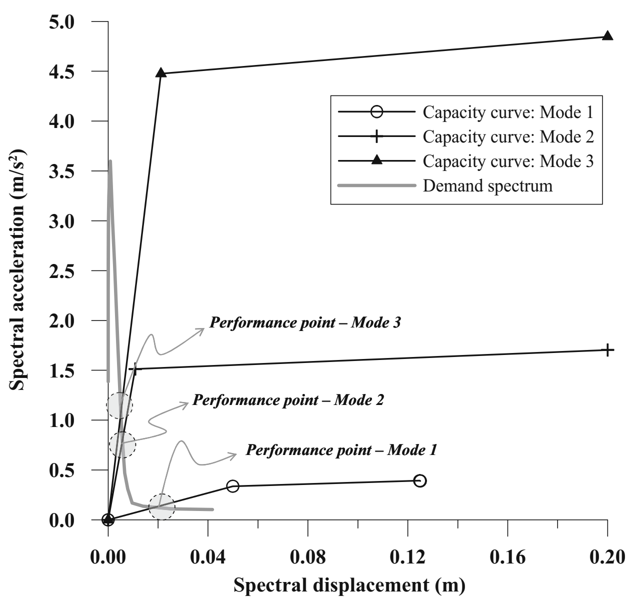

Figure 10. Estimation of the performance points or seismic demand for the three modes from the intersection of the demand spectrum and respective capacity curves.

the seismic demand for each mode (figure 10). All three capacity curves intersect the demand curve within the elastic range, thereby avoiding iteration to obtain the performance point. Then, response from each mode was combined by SRSS to obtain the peak response. Results of the analysis for the 2475-year return period are compared to those from NTHA.

4.4b *Non-linear dynamic analysis*: The lumped mass model was used to perform NTHA with the spectrum-compatible natural records selected for different return periods. Average response quantities have been computed based on the results of the individual NTHA using the suites of accelerograms. Results from the non-linear analyses using recorded motions pertaining to the 2475-year return period are reported in figure 11.

4.5 *Discussion of results*

Different modelling strategies have been used with three different analysis procedures in order to evaluate the seismic vulnerability of the *gopuram*. From the results it evident that the location of maximum stress for seismic loading is near the 7^{th} floor, which could be a potential location for non-linearity to evolve. Subsequently, the cross section at this level was considered to develop a moment-curvature relation, by increasing the eccentricity of axial load from zero until the extreme compression fibre of the section reaches a maximum strain of 0.003. The tensile strength of the masonry was ignored; hence the area under tension is sequentially ignored. The effect is rather conspicuous because of the cross section being rectangular. This non-linear relationship represents the capacity of the section (refer figure 12). When the curvature demand exceeds 7.13E-05/m, the section begins to crack, and when it exceeds 4.54E-04/m, crushing begins.

The MPA curvature demand is above the elastic section capacity but below the cracking limit. The average NTHA curvature demand crosses the cracking limit, but is below the crushing limit. The section begins to crack when the extreme fibres are decompressed. Upon any further increase in lateral load, the crack propagates and continues to widen until it jeopardizes the stability of the tower. Though initiation of damage arises from tensile stress, the ultimate failure is caused by exceedance of compressive strength of the extreme fibre. MPA is apparently effective in capturing higher mode contributions, and response quantities are comparable with those from NTHA.

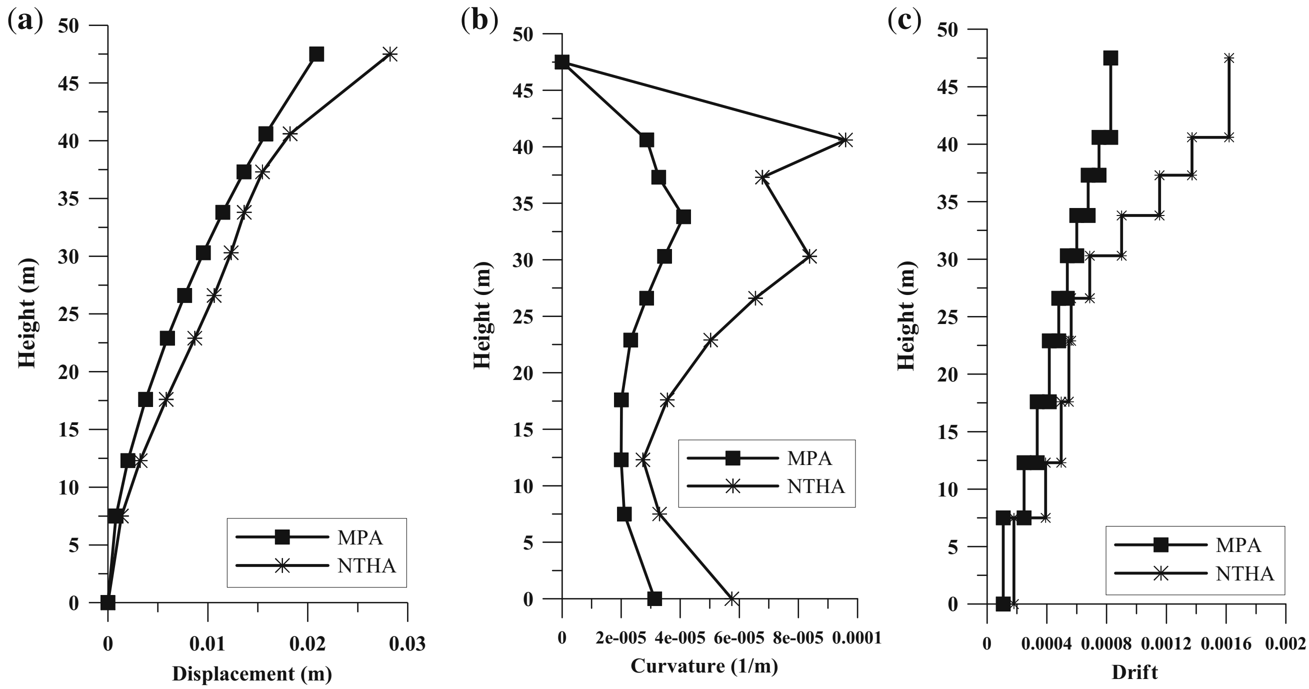

Figure 11. Average (**a**) displacement, (**b**) curvature and (**c**) drift profiles from the non-linear time-history analyses compared to the results of the modal pushover analysis.

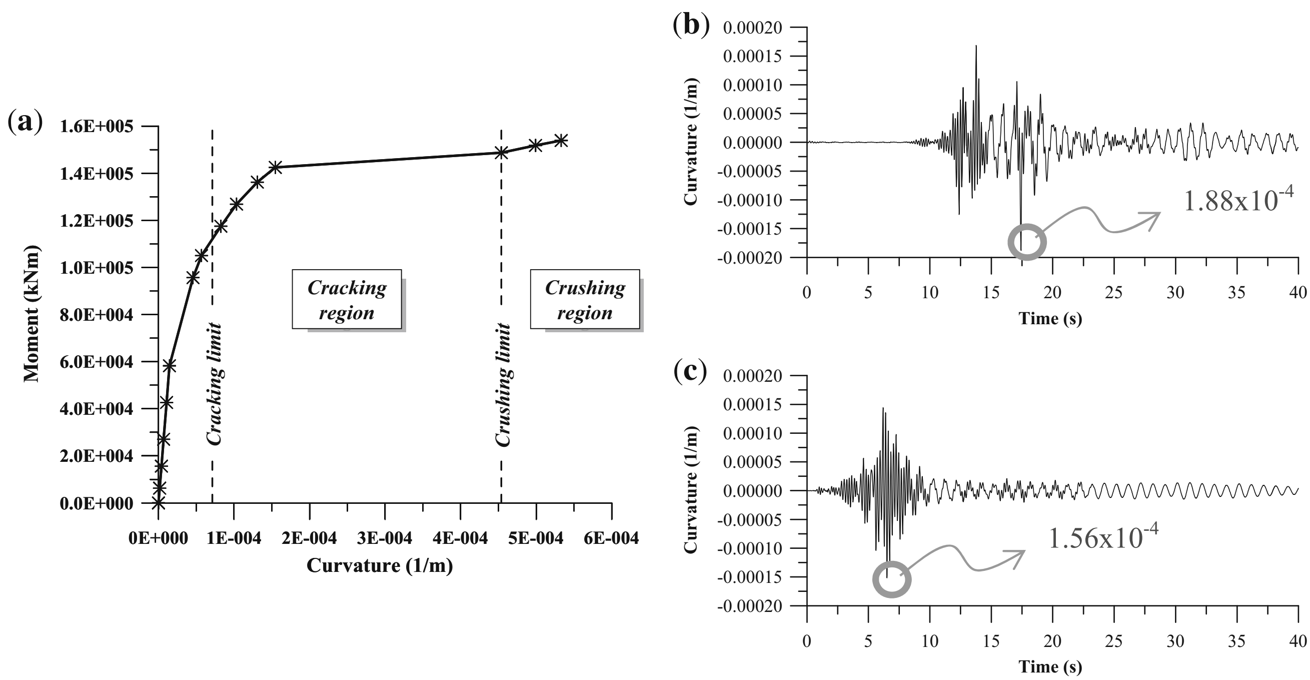

Figure 12. (**a**) Moment-curvature relationship developed for the cross section at 7th storey of the *gopuram*; Curvature history at 7th storey section (**b**) record 2 and (**c**) record 4 from the non-linear time-history analyses showing sectional curvature values beyond the estimated cracking limit.

The following inferences can be drawn:

- Lime mortar is heavily used in a *gopuram*. Though it possesses lower strength, its deformation capacity is higher compared to other binding materials; hence, the structure can be expected to have more energy dissipation capacity, which is favourable against dynamic loading.

- The failure of the structure evolves from material failure, and instability should not be an issue because of its favourable configuration (pyramidal). The natural frequency (1.30-1.60 Hz) is well-separated from the fundamental soil frequency (3.48-3.79 Hz), indicating no possibility of resonance.
- Response spectrum analyses suggest that tensile stresses can be expected in the upper parts of the *gopuram* for 975 and 2475-year return period ground motion (very rare events). in the latter, tensile stress beyond the conventional limit of 0.1 MPa was observed at the 7^{th} storey level.
- In agreement with linear dynamic analysis, both static (MPA) and dynamic non-linear analyses (NTHA) indicate non-linear deformations at the 7^{th} storey. Hence, it is evident that the upper levels of the structure are more vulnerable than the base, where a concentration of curvature is expected (see figure 12(b)–(c). This is attributable to an unfavourable combination of reduced cross-sectional area, low axial compressive stress and higher mode effects.
- MPA approach captures the non-linear behaviour of the tower efficiently in comparison to conventional pushover analyses. However, due to low level of inelastic demand in the current case, there is insufficient ground to conceive MPA as an alternative to NTHA, when seismic input is unavailable in an appropriate form (i.e., natural records).
- The survival of such structures in the region over the centuries can be attributed to the low historical seismicity (relatively low magnitude earthquakes at long distances) from the archaeological site.

5. Analysis of the *mandapam*

5.1 *Ambient vibration tests*

Ambient vibration tests provide a useful check on the natural frequencies of the structure as predicted by the FE model. The ambient vibrations of the 4- and 16-pillared short *mandapams* at Ekambareswar temple were recorded using a digital seismograph. A Lennarz 3D/5s geophone was used as a transducer, while data acquisition was carried out with an A/D PCMCIA National Instruments (16-bit resolution, maximum sampling rate 200 kHz). The sensitivity of the 3D/5s is 400 V7 (m/s) in the frequency band 0.2-100 Hz. Data acquisition was using single receiver points, recording few minutes of ambient vibrations, avoiding as much as possible, any movement or vibration close to the receiver. The data was processed by computing amplitude spectra, and the ratio between the horizontal and vertical components. It was concluded that the dominant frequency of 2.5 Hz is the main natural frequency of the 16-pillared *mandapam*, and 3.6 Hz as that of the 4-pillared *mandapam*, associated to horizontal motion (figure 13(a)-(b).

5.2 *Structural modelling*

5.2a *3D finite element model*: An FE model was developed in ABAQUS 6.6.4, with tetrahedron (C3D10) and brick (C3D20) elements. Pillars were modelled with their effective cross section, with the decorative carving ignored. The roof system was modelled, and the parapet was accounted only as mass. The foundation was not modelled due to its limited dimensions. The dynamic soil behaviour was simulated using equivalent springs as described earlier.

5.2b *Modal analysis*: The structure has symmetrical vibration modes due to its symmetry in plan, except for the 16-pillared tall *mandapam*, where few pillars are rectangular in cross-section. The nature of the first three modes is similar in all the *mandapams* investigated, the first two associated with bending in the principal directions and the third, torsional. The mass associated with the torsional mode is negligible due to symmetry. The dynamic properties are reported in table 7 and mode shapes in figure 15. Unlike the rocking-cum-sliding mode of vibration in classical multi-drum columned structures [12], flexibility introduced by slender monolithic pillars makes such modes of vibration unviable in the *mandapam* (figure 14).

5.2c *Response spectrum analysis*: The structure has been analysed for seismic input pertaining to different return periods. Stresses from the response spectrum analysis were combined with the stresses from gravity loads to calculate the resultant stress due to the load combination. Only tensile stresses from the response spectrum analyses have been considered in view of the high compressive strength of the material.

The stress contours due to the seismic load are illustrated in figure 15(a)–(d). Resultant tensile stresses due to a combination of gravity and seismic loads for different return periods are shown in figure 16. The seismic response of these structures is sensitive to their fundamental frequency. The short *mandapams* have higher fundamental frequencies, placing them in the high response region of the spectrum compared to the taller *mandapams*. For ground motion pertaining to the 95-year return period, none of the structures develop tensile stress. Their survival in spite of several seismic events of low magnitude in the past corroborates the above result. However, under ground motion with longer return periods (475, 975 and 2475 years), all the four models develop significant tensile stresses, which could invalidate the linear elastic model.

5.3 *Limit analysis*

Linear elastic analysis requires data on elastic material properties and the maximum permissible stress, and

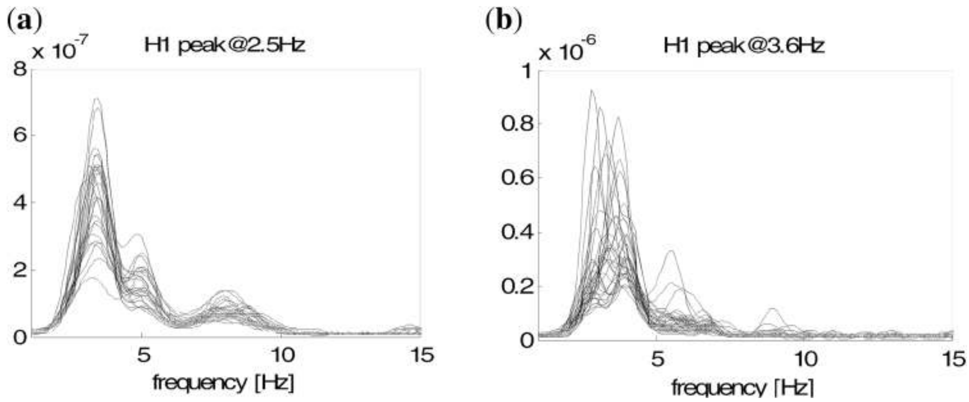

Figure 13. (**a**) Amplitude spectra for ambient vibration tests on the 16-pillared mandapam; (**b**): amplitude spectra for ambient vibration tests on the 4-pillared *mandapam*.

Table 7. Dynamic properties of the *mandapams* from 3D FE model.

			Effective Modal Mass			Cumulative Modal Mass		
Mode No	Frequency (Hz)	Mode of Vibration	Ux	Uy	Uz	Ux	Uy	Uz
4-pillared *mandapam*								
1	3.53	B-YY	0.26	0.65	0.00	0.26	0.65	0.00
2	3.54	B-XX	0.65	0.26	0.00	0.91	0.91	0.00
3	5.10	T	0.00	0.00	0.00	0.91	0.91	0.00
4	23.92	ZZ	0.00	0.00	0.88	0.91	0.91	0.88
16-pillared *mandapam*								
1	3.46	B-YY	0.16	0.77	0.00	0.16	0.77	0.00
2	3.47	B-XX	0.77	0.16	0.00	0.93	0.93	0.00
3	4.02	T	0.00	0.00	0.00	0.93	0.93	0.00
4	20.54	ZZ	0.00	0.00	0.90	0.93	0.93	0.90
4-pillared *mandapam* (Tall)								
1	1.73	B-YY	0.15	0.79	0.00	0.15	0.79	0.00
2	1.73	B-XX	0.79	0.15	0.00	0.94	0.94	0.00
3	2.40	T	0.00	0.00	0.00	0.94	0.94	0.00
4	12.46	ZZ	0.00	0.00	0.91	0.94	0.94	0.91
16-pillared *mandapam* (Tall)								
1	2.10	B-YY	0.00	0.96	0.00	0.00	0.96	0.00
2	2.69	B-XX	0.95	0.00	0.00	0.95	0.96	0.00
3	2.80	T	0.00	0.00	0.00	0.95	0.96	0.00
4	13.40	B-YY	0.00	0.00	0.16	0.95	0.96	0.16
5	13.80	B-XX	0.00	0.00	0.00	0.95	0.96	0.16
6	15.03	ZZ	0.00	0.00	0.45	0.95	0.96	0.61

NOTE: B-XX – Bending about XX axis; B-YY – Bending about XX axis; T – Torsional; ZZ- Vertical modes

provides information on the deformation behaviour and stress distribution in the structure. The ultimate limit state safety requirement is not satisfied if the strength capacity of even a single element is exceeded. Such a state clearly does not correspond to the ultimate capacity of the system. Under ultimate conditions, moderate non-linear response of masonry structures demonstrates a situation where forces are shared according to strength capacity of sub-structures and not according to their elastic stiffness. In the analysis of historical masonry structures, therefore, the approach of limit analysis is suitable even for horizontal loads simulating seismic forces. Limit analysis requires data on the strength of materials, and provides information on the failure mechanism of the structure, and evaluates the structural load at mechanism formation. Once tensile stresses are encountered, linear elastic analysis is unreliable in predicting the response of masonry structures.

Limit analysis is based on three assumptions: (1) infinite compressive strength of the material, (2) zero tensile strength, and (3) collapse is due to instability of the system,

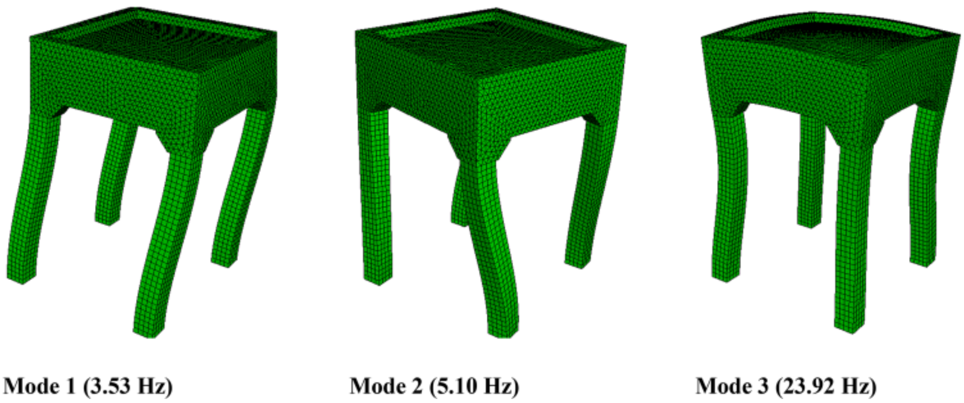

Figure 14. First three mode shapes and frequencies obtained from the 3D FE model of the short 4-pillared mandapam.

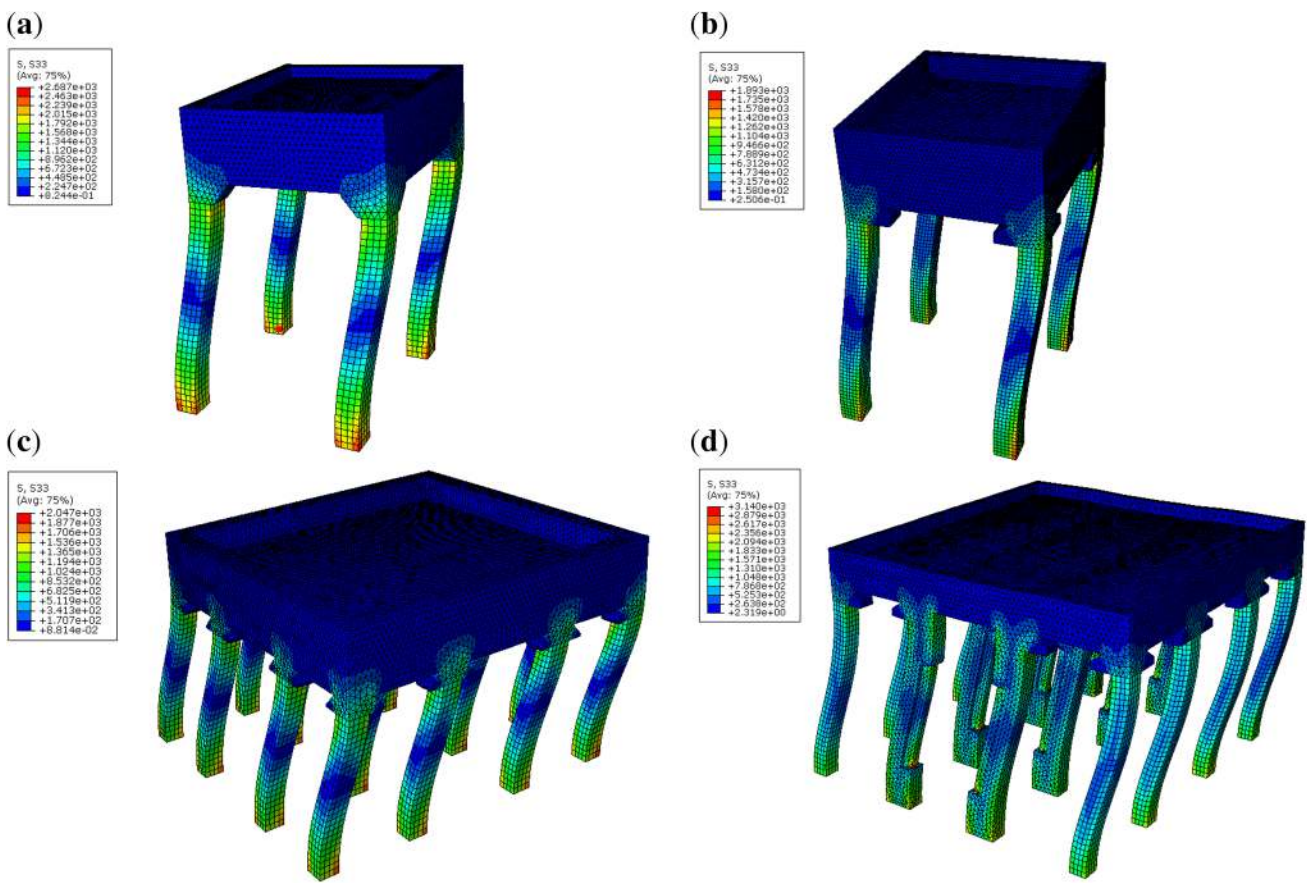

Figure 15. Stress contours from response spectrum analyses: (**a**) 4-pillared short *mandapam*; (**b**) 4-pillared tall *mandapam*, (**c**) 16-pillared short; (**d**) 16-pillared tall *mandapam* (units: KPa).

caused by minimum displacement rather than exceedance of a threshold stress level. Collapse is normally partial involving sub-structures or components. When horizontal accelerations are high enough to trigger a mechanism, different structural components can be idealized as rigid bodies. The lateral force capacity of this subsystem can be related to an acceleration, and the static threshold resistance can be evaluated through equilibrium limit analysis and application of the principle of virtual work. The structure is considered to be an assembly of beams and columns, and the connection between elements can be lost under seismic loading. The seismic vulnerability of the *mandapams* mainly evolves from the lack of integral connection, in addition to the slenderness effect of pillars, which

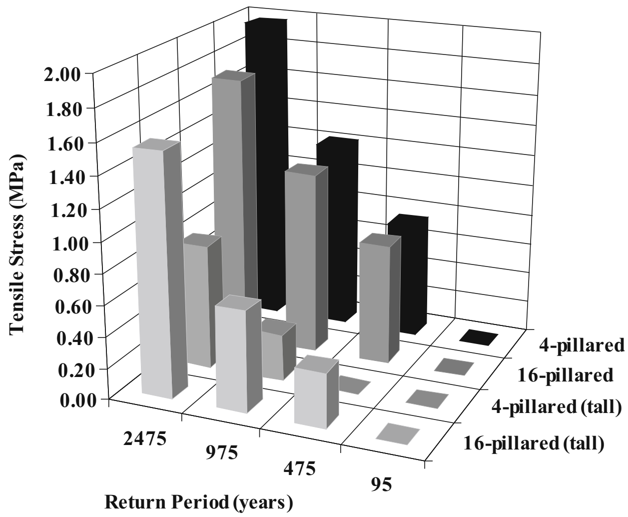

Figure 16. Stress resultants from the seismic and gravity loading for the *mandapams*.

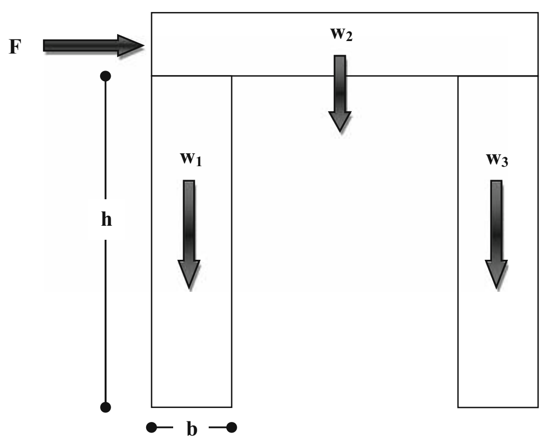

Figure 17. Structural idealisation of the *mandapam*.

ultimately triggers instability in the system. Therefore, a simple stability check has been carried out for sliding and overturning mechanisms. The three potential collapse mechanisms could be enumerated as follows: (a) overturning of two pillars, (b) sliding of the roof and (c) sliding of the pillars.

5.3a *Calculation of lateral forces*: The *mandapam* is idealised as an SDOF plane structure, illustrated in figure 17, which is valid because the symmetric structure derives its lateral stiffness from its pillars, and the principal mass from its roof. Modal analysis also supports such an SDOF idealization (mass participation of the fundamental modes is greater than 90%, and higher mode effects are negligible). The base shear, V, was calculated based on the equivalent static approach, i.e., self-weight, W, is multiplied by a coefficient (α), which essentially is spectral acceleration, and depends on the frequency of the structure, as well as the PGA expected at the site.

$$\begin{aligned} V = \alpha(W_1 + W_2 + W_3) = F \\ \alpha = V/W \end{aligned} \tag{1}$$

5.3b *Mechanism of overturning of pillars*: The first mechanism that could be triggered is the overturning of multiple pillars, as shown in figure 18(a)-(b). Under ideal conditions, the collapse of structure occurs due to the overturning of the entire structure. In the absence of integral connection between beam and pillars, the resistance to overturning is offered merely by the pillars. The resisting moment is given by the product of weight carried by the pillar and half of its width (b/2). The trend of the factor of safety (FOS) with respect to PGA, where FOS is the ratio between the lateral capacity coefficient, β, and the base shear coefficient, α, is shown in figure 19. Given the lack of positive interconnection between the pillars and the roof (deteriorated mortar joint in ancient structures and lack of dowels), overturning mechanism could be the governing collapse mode.

$$\begin{aligned} F\theta h = 0.5W_1\theta b + W_2\theta b + 0.5W_3\theta b \\ F = 0.5b(W_1 + 2W_2 + W_3)/h \\ \beta = 0.5b(W_1 + 2W_2 + W_3)/Wh \\ FOS = \beta/\alpha \end{aligned} \tag{2}$$

5.3c *Mechanism of sliding of roof*: Lateral action tries to slide the structure or a part of the structure and such a sliding mechanism could be resisted by frictional forces at the sliding interface. It is assumed that the resistance offered by the mortar connection is negligible. Among possible mechanisms for sliding, the sliding of the roof (refer figure 18(c)-(d) and the sliding of the entire structure (refer fig. 18(e)-(f) were treated as two alternatives. It is seen that safety against sliding is much higher compared to that against overturning. Similar inferences have been reported in the literature too [12, 14]. The results also reveal that sliding can take place even if the base shear coefficient is less than the coefficient of friction, μ. The frictional coefficient for the study was assumed to be 0.4 (granite sliding on granite) and Δ is the finite displacement.

$$\begin{aligned} F\Delta = W_2\mu\Delta \\ FOS = W_2\mu/(\alpha W) \end{aligned} \tag{3}$$

5.3d *Mechanism of sliding of whole structure*: The sliding of the whole structure may have a scant possibility of occurrence because of the high value of coefficient of friction. Nevertheless, this was also considered.

$$\begin{aligned} F\Delta = (W_1 + 0.5W_2)\mu\Delta + (W_2 + 0.5W_3)\mu\Delta \\ FOS = \mu/\alpha \end{aligned} \tag{4}$$

5.3e *Parametric study*: For a more generalised assessment procedure, a parametric analysis was carried out by considering ranges for the variables that influence the safety of these structures. The cross-sectional dimensions and height

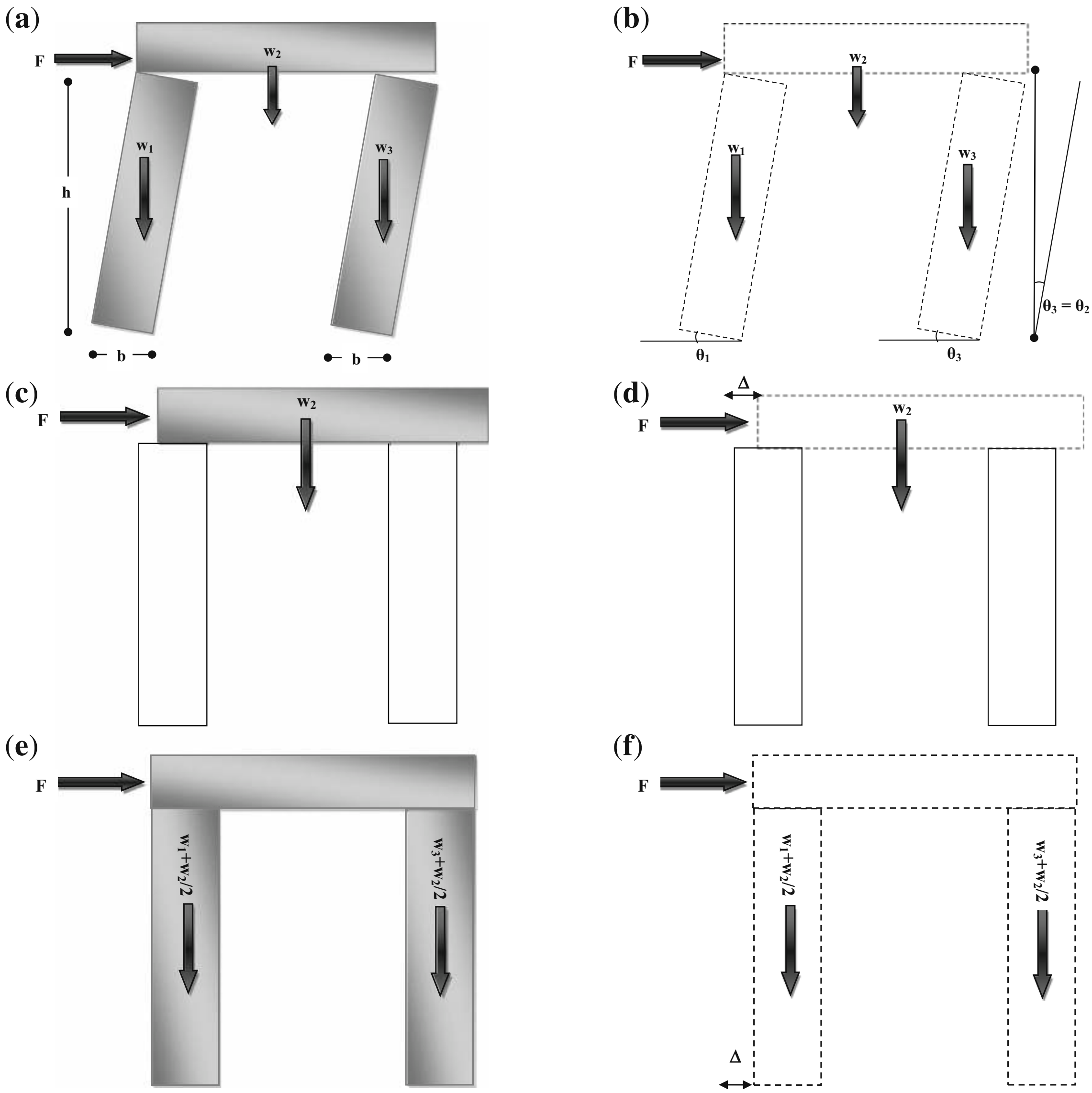

Figure 18. Idealisation of mechanisms: I-II-III (**a-c-e**) loads and geometry; (**b-d-f**) kinematic action.

of the structure significantly influence the collapse mechanism. The governing failure criterion is due to mechanism I. A range of possible widths and heights were considered as parameters and their safety was evaluated for a range of PGAs for mechanism I (see figure 20). Wider pillars imply higher factor of safety against overturning, but the lateral capacity coefficient, β, and consequently, FOS decrease with increasing height.

5.4 *Discussion of results*

Under seismic ground excitation, the *mandapam* structure is subjected to cyclic lateral forces, With the assumption of no tensile strength of mortar, collapse of the structure can be triggered by instability, either from overturning or sliding of the structural members. Linear elastic response spectrum analyses on 3D FE models of the *mandapam* showed how tensile stresses can be expected at the base of the pillars (figure 16).

From limit analysis and with reference to figure 19 (a)-(d), it is clear that the overturning mechanism governs. The sliding mechanisms (particularly, of the entire structure) has significantly higher FOS against collapse. From the limit analysis, with reference to figure 21, we see that at a PGA of 0.04 g, the FOS for all the four *mandapams* is greater than 1.0. This is consistent with the inference from the linear elastic analysis that tensile stress may not develop at the base of the pillars under a combination of seismic excitation for the 95-year return period and gravity load. Therefore, clearly at this level of ground acceleration, no mechanism can be triggered. An

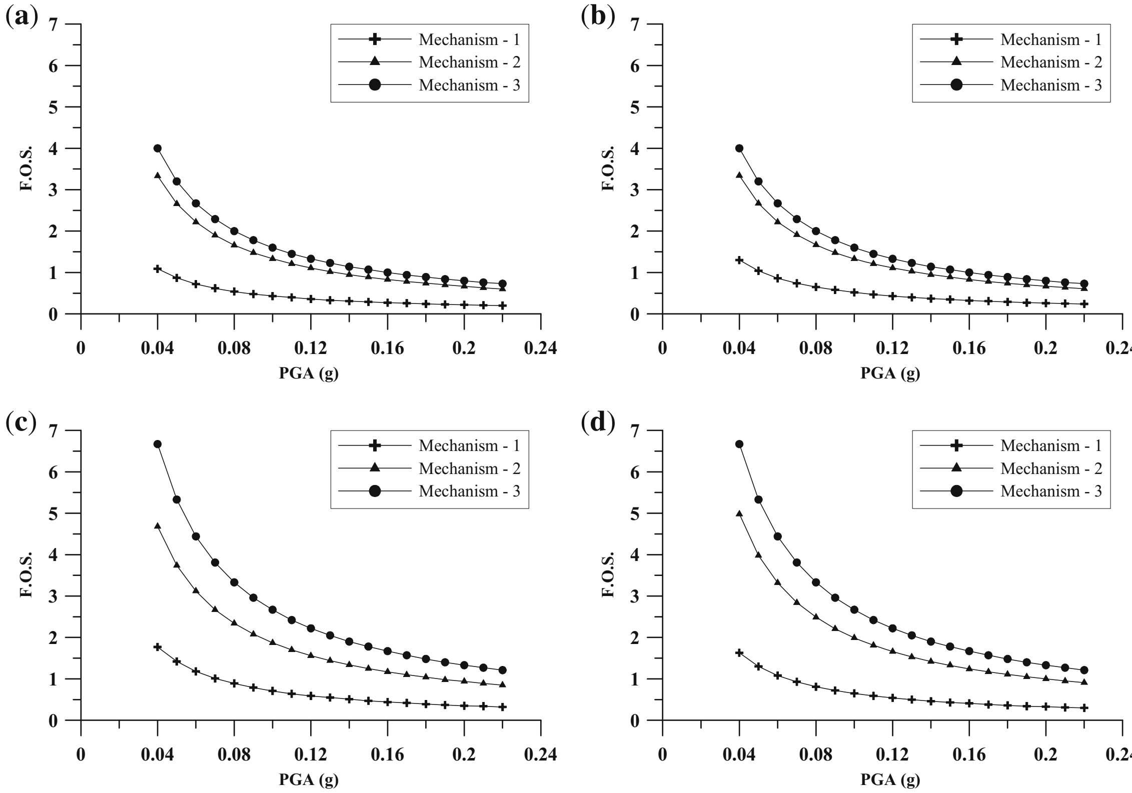

Figure 19. Check for stability: (**a**) 4-pillared short mandapam; (**b**) 16-pillared short mandapam; (**c**) 4-pillared tall *mandapam* and (**d**) 16-pillared tall *mandapam*.

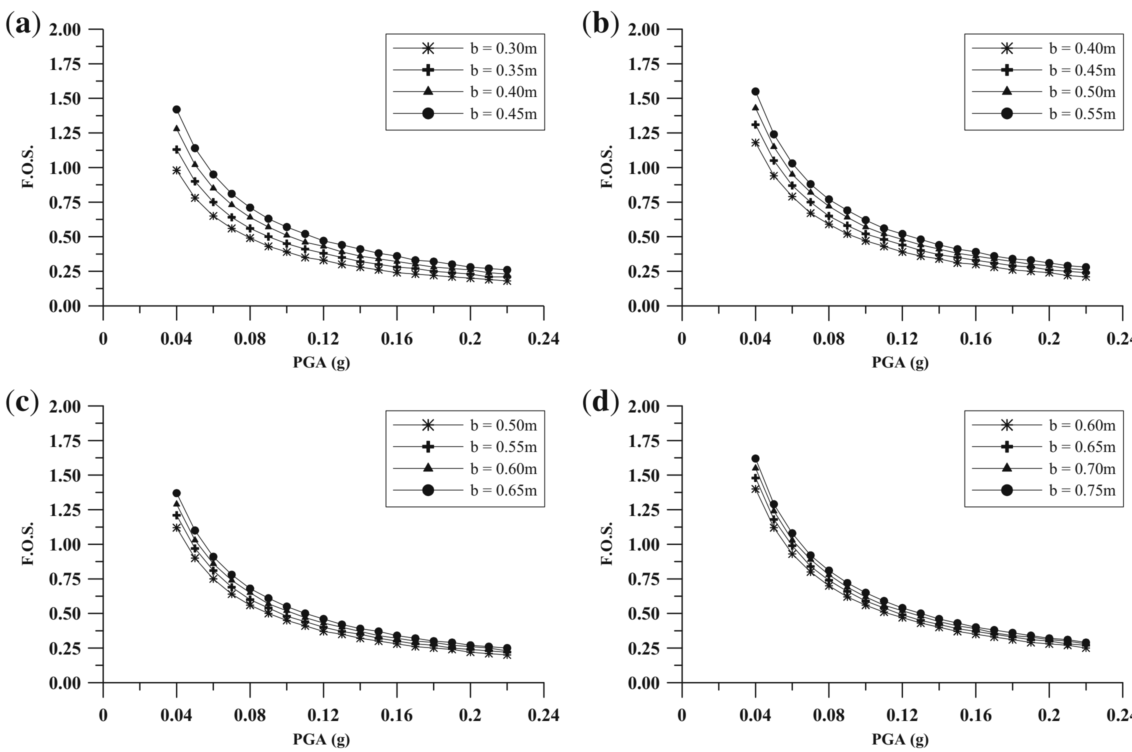

Figure 20. Parametric study on influence of pillar height and cross-sectional width on safety factors estimated for the overturning mechanism: (**a**) pillar height 3 m; (**b**) pillar height 4 m; (**c**) pillar height 5 m and (**d**) pillar height 6 m.

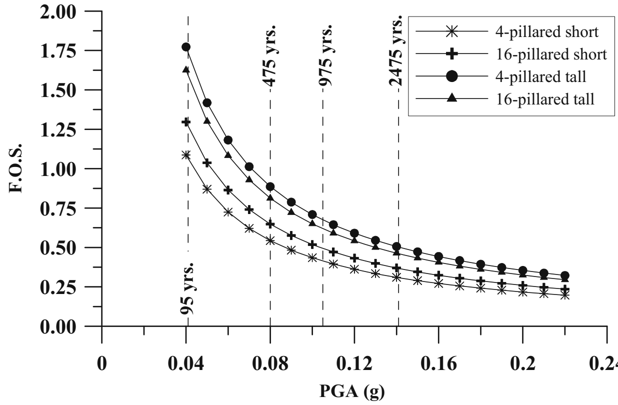

Figure 21. Comparison of F.O.S. trends from overturning mechanism for the 4 *mandapams* to PGA corresponding to return periods (95. 475, 975 and 2475 years).

FOS slightly less than 1.0 for the overturning mechanism is seen for a PGA of 0.08 g for the 4-pillared tall *mandapam*. According to the linear elastic analysis, tensile stress should not be expected at the base of the pillars even for this level of PGA. The decompressed state of the extreme fibre in a cross section of a structural member could be the inception of a mechanism within a rigid body idealisation. Collapse is ultimately due to instability. However, beyond the initiation of cracking, linear elastic analysis fails to adequately represent the structural behaviour, especially in historical masonry.

The inferences from the present investigation on *mandapam* are in line with the conclusions of similar studies in the literature [12, 14, 15, 36]. Some of the salient inferences can be enumerated as follows.

- The current study, like others in the literature e.g., [15], suggests that FE approach for modelling the seismic response of dry historical masonry structures may not be appropriate, and results from FE approach can be misleading unless they are properly interpreted. This could be an effective tool if FE models are validated with appropriate field testing for dynamic identification.
- The structure could be sensitive to ground motion parameters (especially frequency content, as seen in the case of the short 4-pillared *mandapam*). Psycharis [36] point out that the period of the ground excitation will have a significant effect on the threshold acceleration and mode of collapse and that high frequency motion is much more dangerous for dry masonry columned structures.
- The survival of similar structures in the region over several centuries could be attributed to the relatively low seismicity of the region, as inferred in the case of the *gopuram*. These structures seem to be capable of resisting low return period ground motion (e.g., no tensile stress in 95-year return period ground motion). Numerical simulations on column-architrave structures [11] have shown that significant permanent deformation occurs only for ground motion with PGA $\sim$ 0.6 g. However, the frequency of the excitation is a very important indicator of the vulnerability.
- Shorter *mandapam* can be more vulnerable than taller ones as they are stiffer, with their frequencies falling in the plateau of the response spectrum. The supporting pillars are not very wide and this increases their vulnerability as evinced from the parametric study using limit analysis approach.
- The collapse of the structure is due to instability of the system. The identified collapse mechanisms are overturning and sliding mechanisms, and limit analysis reveals that the former always governs. This is attributable to the fact that sliding resistance is a function of the coefficient of friction (μ for granite is around 0.4-0.6), whereas overturning resistance depends on the geometry of the structure. Lack of positive connection (dowels) and presence of weak mortar joints between structural members, and the slenderness of pillars make the structure vulnerable to lateral loads.

6. Conclusions

Structural analysis of historical constructions is carried out for a better understanding of structural behaviour and/or to be able to arrive at residual capacity while carrying out structural assessment and to arrive at a strengthening strategy, if warranted. Since the subject of conservation is predominantly steered by archaeologists and architects, seldom a quantitative approach is adopted. Engineers also are reluctant in analysing such structures due to the inapplicability of modern structural standards to these structures. In this context, the research presented in this article demonstrates the possibility of a quantitative approach even for historical constructions. The adopted methods have to be chosen, essentially with recourse to first principles, and the outcome undoubtedly requires validation for reliable application. Experimental validation, expect for the use of measured fundamental frequency of the *mandapam* to adopt the right type of model, is beyond the scope of the current research. When it comes to modelling massive constructions in historical masonry, it has been observed that structural geometry, including boundary conditions overrides material strength in being able to predict the structural behaviour, which is particularly true for historical masonry [37].

An initial attempt at understanding the seismic behaviour of the *gopuram* and the *mandapam*, monumental structures representative of Dravidian temple architecture is presented. Different analysis approaches lead to comparable inferences on the seismic response of the *gopuram*, despite significant idealisation. Non-linear deformations due to seismic loading can be expected at the 7th storey level under ground motion corresponding to a 2475-year return period (PGA 0.14 g), whereas response should be essentially elastic under the 475-year return period earthquake (PGA 0.08 g). Collapse of such a structure would primarily be due to material failure; i.e., increasing load eccentricity would lead to progressive cracking of the section due to tensile stresses, and consequent compression failure of extreme section fibres.

With regard to the seismic assessment of the *mandapam,* the study reveals that the vulnerability of the *mandapam* is mainly due to the lack of proper interconnection between structural members. Recourse to limit analysis to model the *mandapam* was made owing to the unrealistic behaviour resulting by the deformable continuum in the FE models. Collapse due to overturning mechanisms will govern its response under seismic loading. The short 4-pillared *mandapam* is apparently the most vulnerable. The accentuated response under seismic excitation is attributed to its high fundamental frequency.

The role of seismic retrofitting of a mandapam is to ensure interconnection between structural members, thereby making the structure safe against earthquakes. As far as retrofitting of heritage structures are concerned, the intervention has to be minimal, fully reversible and it should not adversely affect aesthetics. Integral action can be ensured by inserting stainless steel or titanium dowels connecting the beams, corbels and pillars. However, some important remarks made by others researches [11, 12] regarding the applicability of this procedure to multi-drum temples in Greece are noteworthy: (a) this approach does not improve the response significantly, and (b) inserting the rods rules out the possibility of sliding which play a major role in increasing the damping (due to friction). Nevertheless, the insertion of a stiff element between components of the *mandapam* might play a better role compared to multi-drum classical columns. This approach has to be adequately verified with numerical and laboratory studies before any recommendations can be given.

Acknowledgements

Seismic vulnerability assessment of monumental structures at the archaeological site of Ekambareswar temple, Kancheepuram was carried out within the framework of a 3-year research project funded by the Department of Science and Technology, Government of India and Ministry of Foreign Affairs, Italy, entitled '*Seismic Risk Assessment of Historical Centres in South India*' in collaboration with Indian Institute of Technology Madras and University of Pavia, Italy. The role of the Governmental Institutions is greatly appreciated.

References

[1] Riva P, Perotti F, Guidoboni E and Boschi E 1998 Seismic analysis of the Asinelli tower and earthquakes in Bologna. *Soil Dyn. Earthq. Eng.* 17: 525550

[2] Menon A, Lai C, Macchi G and Pavese A 2006 Non-linear dynamic analyses for seismic assessment of ancient masonry towers. In: *Proceedings of V International Conference on Structural Analysis of Historical Constructions* (ed. Lourenço, P.B. *et al*), New Delhi, India

[3] Jaishi B, Ren W-X, Zong Z-H and Maskey P N 2003 Dynamic and seismic performance of old multi-tiered temples in Nepal. *Eng. Struct.* 25(14): 1827–1839

[4] Peña F, Lourenço P B and Mendes N 2008 Seismic assessment of the Qutb minar in Delhi, India. In: *Proceedings of 14th World Conference on Earthquake Engineering*, October 12-17, 2008, Beijing, China

[5] Sezen H, Acarb R, Dogangunb A and Livaoglu R 2008 Dynamic analysis and seismic performance of reinforced concrete minarets. *Eng. Struct.* 30(8): 2253–2264

[6] Dogangun A, Acar R, Sezen H, Livaoglu R 2008 Investigation of dynamic response of masonry minaret structures. *Bull. Earthq. Eng.* 6(3): 505–517

[7] Clemente P, Saitta F, Buffarini G, Platania L 2015 Stability and seismic analyses of leaning towers: The case of the minaret in Jam. *Struct. Des. Tall Spec. Build.* 24(1): 40–58

[8] Mahalingam T V 1970 XII. Engineering - The south Indian temple - Medium of construction. *Indian. J. History of Science*, 5(2): 309–314

[9] Grover S 1980 *The architecture of India: Buddhist and Hindu*. New Delhi: Vikas Publishing House Pvt. Ltd.

[10] D'Ayala D and Kansal A 2004 An analysis of the seismic vulnerability of the architectural heritage of Bhuj, Gujarat, India. In: *Proceedings of Structural Analysis of Historical Constructions*, Modena C, Lourenço P B and Roca P (eds.), pp. 1069–1078

[11] Psycharis I N, Lemos J V, Papastamatiou D Y, Zambas C and Papantonopoulos C 2003 Numerical study of the seismic behaviour of a part of the Parthenon Pronaos. *Earthq. Eng. Struct. Dyn.* 32(13): 2063–2084

[12] Konstantinidis D and Makris N 2005 Seismic response analysis of multi-drum classical columns. *Earthq. Eng. Struct. Dyn.* 34(10): 1243–1270

[13] Ambraseys N and Psycharis I N 2011 Earthquake stability of columns and statues. *J. Earthq. Eng.* 15(5): 685–710

[14] Giordano A, De Luca A, Mele E and Romano A 2007 A simple formula for predicting the horizontal capacity of masonry portal frames. *Eng. Struct.* 29(9): 2109–2123

[15] Maeda T, Sugiura Y and Hirai T 2008 FEM modeling of the towers in Bayon temple in Cambodia based on micro-tremor measurements. *Adv. Eng. Softw.* 39(4): 346–355

[16] Lourenço P B and Roque A 2006 Simplified indexes for the seismic vulnerability of ancient masonry buildings. *Constr. Build. Mater.* 20(4): 200–208

[17] IS-1893-Part 1, 2002 *Indian standard criteria for earthquake resistant design of structures*, 5th Revision. New Delhi: Bureau of Indian Standards

[18] Lai C G, Menon A, Corigliano M, Ornthamarrath T, Sanchez H L and Dodagoudar G R 2009 Probabilistic seismic hazard assessment and stochastic site response analysis at the

archaeological site of Kancheepuram in Southern India. In: *Research Report EUCENTRE 2009/01,* IUSS Press, Pavia, p. 250

[19] Corigliano M, Lai C G, Menon A, Ornthammarath T 2012 Seismic input at the archaeological site of Kancheepuram in Southern India. *Nat. Hazards* 63(2): 845–866

[20] Dall'Ara A, Lai C G and Strobbia C 2006 Selection of spectrum-compatible real accelerograms for seismic response analyses of soil deposits. In: *Proceedings of 1st European Conference on Earthquake Engineering and Seismology*, Geneva, Switzerland

[21] CEN-EN 1998-1, 2005 Eurocode-8: *Design of structures for earthquake resistance: Part 1: General rules for seismic action and rules for buildings*. European Committee for Standardization, Brussels

[22] Gazetas G 1991 Ch. 15: Foundation vibrations. In: *Foundation Engineering Handbook*, Fang HY (ed.). Van New York: Nostrand Reinhold, pp. 553–593

[23] Kaushik H B, Rai D C and Jain S K 2007 Stress-strain characteristics of clay brick masonry under uniaxial compression. *J. Mater. Civ. Eng. ASCE* 19(9): 728–739

[24] Gumaste K S, Nanjunda Rao K S, Venkatarama Reddy B V and Jagadish K S 2007 Strength and elasticity of brick masonry prisms and wallettes under compression. *Mater. Struct.* 40: 241–253

[25] Sarangapani G, Venkatarama Reddy B V and Jagadish K S 2002 Structural characteristics of bricks, mortar and masonry. *J. Struct. Eng. (India)* 29(2): 101–107

[26] Pande G N, Liang J X and Middleton J 1989 Equivalent elastic moduli for brick masonry. *Comput. Geotechn.* 8: 243–265

[27] Casolo S 2001 Significant ground motion parameters for evaluation of the seismic performance of slender masonry towers. *J. Earthq. Eng.* 5(2): 187–204

[28] Casolo S and Peña F 2007 Rigid element model for in-plane dynamics of masonry walls considering hysteretic behaviour and damage. *Earthq. Eng. Struct. Dyn.* 21(2): 193–211

[29] Jaishi B, Ren W-X, Zong Z-H and Maskey P N 2003 Dynamic and seismic performance of old multi-tiered temples in Nepal. *Eng. Struct.* 25(14):1827–1839

[30] Peña F, Lourenço PB and Mendes N 2008 Seismic assessment of the Qutb minar in Delhi, India. In: *Proceedings of 14th World Conference on Earthquake Engineering*, October 12-17, 2008, Beijing, China

[31] Menon A, Lai C G and Macchi G 2004 Seismic hazard assessment of the historical site of Jam in Afghanistan and stability analysis of the minaret. *J. Earthq. Eng.* 8(Sp. 1): 251–294

[32] IS 1905 1987 *Code of practice for structural use of unreinforced masonry*. New Delhi: Bureau of Indian Standards

[33] SeismoSoft 2008 SeismoStruct (version 4.0.9) – *A computer program for static and dynamic nonlinear analysis of framed structures (online)*. Available from URL: http://www.seismosoft.com

[34] Chopra AK and Goel RK 2002 A modal pushover analysis procedure for estimating seismic demands for buildings. *Earthq. Eng. Struct. Dyn.* 31: 561–582

[35] Fajfar P 1999 Capacity spectrum method based on inelastic demand spectra. *Earthq. Eng. Struct. Dyn.* 28: 979–993

[36] Psycharis I N, Papastamatiou D Y and Alexandris A P 2000 Parametric investigation of the stability of classical columns under harmonic and earthquake excitations. *Earthq. Eng. Struct. Dyn.* 29(8): 1093–1109

[37] Heyman J 1995 *The stone skeleton: Structural engineering of masonry architecture*. UK: Cambridge University Press, p. 172